Archival Report

Biological Psychiatry

Thalamic Control of Cognition and Social Behavior Via Regulation of Gamma-Aminobutyric Acidergic Signaling and Excitation/Inhibition Balance in the Medial Prefrontal Cortex

Brielle R. Ferguson and Wen-Jun Gao

ABSTRACT

BACKGROUND: The mediodorsal thalamus plays a critical role in cognition through its extensive innervation of the medial prefrontal cortex (mPFC), but how the two structures cooperate at the single-cell level to generate associated cognitive functions and other mPFC-dependent behaviors remains elusive. Maintaining the proper balance between excitation and inhibition (E/I balance) is of principal importance for organizing cortical activity. Furthermore, the PFC E/I balance has been implicated in successful execution of multiple PFC-dependent behaviors in both animal research and the context of human psychiatric disorders.

METHODS: Here, we used a pharmacogenetic strategy to decrease mediodorsal thalamic activity in adult male rats and evaluated the consequences for E/I balance in PFC pyramidal neurons as well as cognition, social interaction, and anxiety.

RESULTS: We found that dampening mediodorsal thalamic activity caused significant reductions in gamma-aminobutyric acidergic signaling and increased E/I balance in the mPFC and was concomitant with abnormalities in these behaviors. Furthermore, by selectively activating parvalbumin interneurons in the mPFC with a novel pharmacogenetic approach, we restored gamma-aminobutyric acidergic signaling and E/I balance as well as ameliorated all behavioral impairments.

CONCLUSIONS: These findings underscore the importance of thalamocortical activation of mPFC gamma-aminobutyric acidergic interneurons in a broad range of mPFC-dependent behaviors. Furthermore, they highlight this circuitry as a platform for therapeutic investigation in psychiatric diseases that involve impairments in PFC-dependent behaviors.

Keywords: Cognition, GABAergic inhibition, Pharmacogenetics, Prefrontal cortex, PVIs, Synaptic function, Thalamus

https://doi.org/10.1016/j.biopsych.2017.11.033

Research on thalamocortical relays has been pivotal in framing our understanding of how sensory information flows from the periphery, to the thalamus, and to its final cortical destination (1). In the medial prefrontal cortex (mPFC), this characterization has been challenging given the complexity of information it receives and must represent in a flexible and dynamic manner. A prime opportunity to advance our understanding of mPFC function is by focusing on the mechanisms of communication with one of its primary gateways, the mediodorsal thalamus (MD). However, despite recent progress (2–4), our grasp on the nature of the interaction between these two structures remains limited.

Cortical neurons are organized into functional micro-columns, where certain columns represent different types of information in a supramodal manner (5,6). Layer III pyramidal neurons (PNs) in the mPFC receive long-range inputs from a wealth of structures, including limbic regions such as the hippocampus and amygdala and neuromodulatory regions such as the ventral tegmental area, locus coeruleus, and dorsal raphe, as well as from the MD (7,8). Layer III PNs can send information horizontally within their lamina as well as synapse onto downstream PNs in layer V (9). Layer V PNs also receive these same long-range inputs from limbic neuromodulatory regions and the thalamus (10,11), along with local inputs from layer III PNs. Using this convergent information, they are tasked with "deciding" whether to fire and transmit a response to downstream motor centers. A state that may aid layer V PNs in performing such calculations is maintaining a high level of gamma-aminobutyric acidergic (GABAergic) inhibition from nearby interneurons relative to excitation (E/I balance) (12).

Two cognitive abilities that are among the most consistently associated with damage to either structure are working memory (WM) (13,14) and cognitive flexibility (15,16). Both represent building blocks of higher-level cognitive processes and are often severely affected in the context of psychiatric disease. In addition, pharmacological studies (17–19) and

SEE COMMENTARY ON PAGE 630

© 2017 Society of Biological Psychiatry.

ISSN: 0006-3223

electrophysiological recordings (20) during behavior suggest that these cognitive domains might be intimately linked to GABAergic signaling in the PFC. Layer III parvalbumin interneurons (PVIs) receive the largest density of innervation from MD fibers (21) and synapse directly on layer V PNs (22). In addition, mPFC PVIs may be more effectively recruited by incoming excitatory stimuli (23), including MD afferents (24). Here, we sought to explore the interplay of these phenomena and demonstrate a causal link among MD hypofunction, mPFC layer V PN E/I balance, GABAergic signaling alterations, and behavioral impairments.

We hypothesized that MD projections provide stronger glutamatergic activation to mPFC PVIs, modulating GABAergic output onto layer V PNs, thereby regulating E/I balance and optimizing mPFC-dependent behavior. Conversely, when thalamic function is compromised, this causes mPFC E/I balance disruption and cognitive dysfunction. To explore this, we used a pharmacogenetic approach to transiently decrease MD activity, induce cognitive impairments, and characterize their mechanistic underpinnings with whole-cell recordings. Following MD silencing, we observed reductions in GABAergic neurotransmission, and a shift in layer V PN E/I balance, concomitant with deficits in WM and set-shifting performance. We used pharmacogenetic and pharmacological approaches, and both restored GABAergic signaling and normalized E/I balance as well as ameliorated select impairments in cognition. Our findings revealed that this pathway is more broadly implicated in other mPFC-dependent behaviors, including social interaction and anxiety, highlighting the importance of thalamocortical activation of mPFC PVIs in a myriad of behaviors.

METHODS AND MATERIALS

Detailed methods are described in the Supplement. Briefly, young adult male Sprague Dawley rats were injected with adeno-associated vectors into the MD (anterior–posterior: −3.3; medial–lateral: 0.7; dorsal–ventral: −5.3) or MD and mPFC (anterior–posterior: 3.2; medial–lateral: 0.5; dorsal–ventral: 2.5). With the exception of those for electrophysiological recordings, all animals were sacrificed for histological confirmation of viral expression. For quantification of the parvalbumin (PV)-hM3D$_q$ virus, mPFC slices from animals injected with the PV-hM3D$_q$-GFP (green fluorescent protein) vector were collected and incubated with primary antibody against PV (rabbit anti-PV, 1:2000; Abcam, Cambridge, MA) and a red fluorescent secondary antibody (DyLight 594–conjugated goat anti-rabbit, 1:500; Jackson ImmunoResearch Laboratories, West Grove, PA).

The WM task was modified from a previous report (25). Briefly, animals were trained to alternate in a T maze following a 10-second delay to obtain a food reward (frosted Cheerios). Animals were injected intraperitoneally 45 minutes prior to each testing day with clozapine-*N*-oxide (CNO; 3 mg/kg), indiplon (1 mg/kg; Tocris Bioscience, Bristol, UK), or an equivalent amount of physiological saline. Groups were compared on days to acquisition and average percentage of correct trials at each delay interval. The set-shifting task was carried out as described in (26). Animals were trained to dig in bowls that varied in either scent (garlic or coriander) or digging medium (sand or bedding). To measure sociability and social novelty, animals were tested in a three-chamber paradigm (27). Anxiety was measured using an elevated plus maze, and time spent in the open versus closed arms was quantified for 5 minutes. Locomotor activity was assessed using an open-field chamber for 15 minutes.

Prior to mPFC whole-cell recordings, viral expression and location were confirmed in MD-containing sections. Electrophysiological parameters were recorded in both current clamp and voltage clamp configurations. For all experiments, to measure the contribution of MD afferent activity to the parameter of interest, we compared the activity of cells with or without CNO (1 or 5 μM). All electrophysiological and behavioral data were analyzed using SPSS Statistics, version 24 (IBM Corp., Armonk, NY). Most measures are presented as mean ± SEM. All procedures involving animals were approved by the Drexel University Institutional Animal Care and Use Committee and conducted in accordance to the National Institutes of Health guidelines.

RESULTS

Expression of Inhibitory Gi-Coupled Designer Receptor Exclusively Activated by a Designer Drug Decreases MD Neuronal Activity

To decrease the activity of MD neurons, rats received a bilateral MD injection (Figure 1A), resulting in expression of the inhibitory hM4D$_i$ designer receptor exclusively activated by a designer drug (DREADD) receptor fluorescently tagged with mCherry (AAV8-CAMKIIα-hM4D(G$_i$)-mCherry [MD-hM4D$_i$]; Figure 1B) or a control virus (AAV8-CaMKIIα-eYFP [yellow fluorescent protein] [MD-YFP]). To confirm the functionality of the hM4D$_i$ receptors, we used whole-cell patch-clamp recordings. The membrane potential of YFP-labeled control cells was not significantly altered by CNO administration (both *p*s $>$ .05; Figure 1C). However, when hM4D$_i$ receptors are bound by CNO, this should activate Gi-mediated signaling and induce hyperpolarization of transfected neurons (28,29). Accordingly, bath application of CNO hyperpolarized hM4D$_i$ neurons (p = .037; Figure 1D), which recovered to baseline following washout ($p > .05$).

CNO Application in the mPFC Reduces Terminal Release From MD Axons

Here, we wanted to assess whether we could use pharmacogenetics as a strategy to evaluate the consequences of downregulating MD activity on individual mPFC neurons. Rats received a bilateral MD transfection with the hM4D$_i$ virus (MD-hM4D$_i$). Following 3 weeks, animals were sacrificed, and mPFC slices were collected (Figure 2A). Given that MD neurons are glutamatergic, we measured the change in spontaneous excitatory postsynaptic currents (sEPSCs) in response to CNO with the goal of decreasing glutamatergic release from severed presynaptic MD terminals in the mPFC. Consistent with previous work demonstrating decreased axonal release (30), CNO significantly reduced the sEPSC frequency in both PNs (p = .012) and fast-spiking interneurons (p = .038) (Figure 2B). In accordance with a presynaptic alteration, the sEPSC amplitudes were not altered ($p > .05$ for both; Supplemental Figure S1B, C). To evaluate whether CNO has

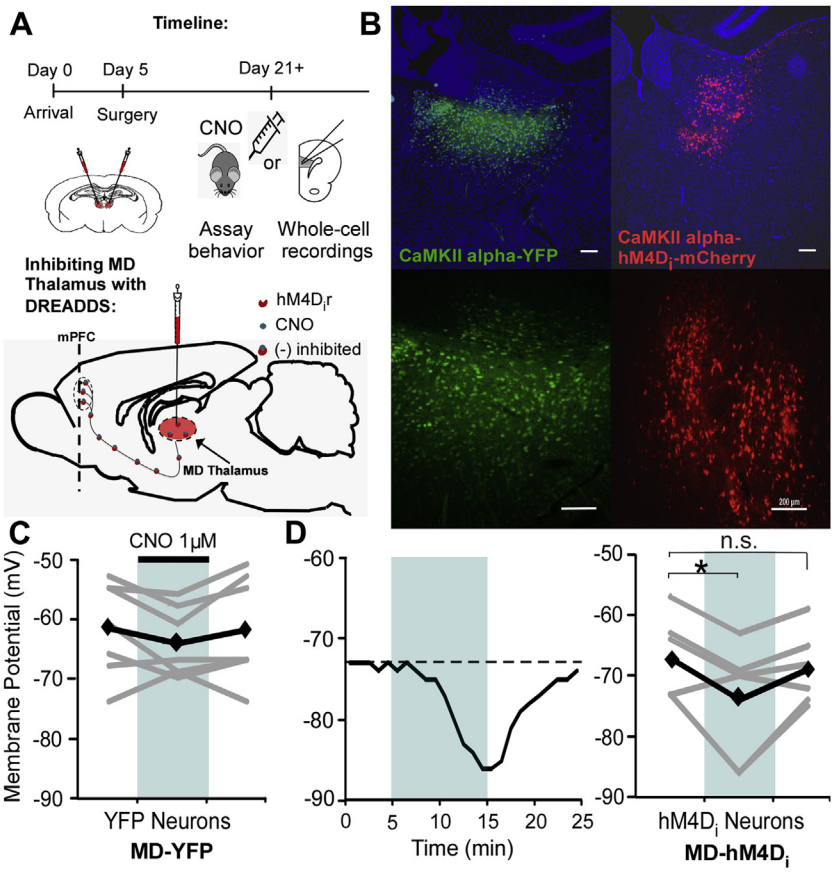


Figure 1. Designer receptor exclusively activated by a designer drug (DREADD) expression and function in the mediodorsal (MD) thalamus. **(A)** Experimental timeline and schematic of viral injection and DREADD approach. **(B)** Expression of the control virus (AAV8-CaMKIIα-eYFP [yellow fluorescent protein]; left) and inhibitory DREADD virus [AAV8-CAMKIIα-hM4D(Gi)-mCherry; right] with 4',6-diamidino-2-phenylindole staining in blue. Scale bar = 200 μm. **(C)** The membrane potential of YFP control cells in the MD did not change in response to 1 μM clozapine-*N*-oxide (CNO) bath application (1 μM, rest = −61.7 ± 3.0 mV; CNO = −64.3 ± 2.2 mV; washout = −62.0 ± 3.3 mV; paired *t* test, both *p*s > .05; *n* = 7). Black represents average, while gray is individual cells. **(D)** Left: Representative response of an $hM4D_i$ neuron to bath application of CNO. Right: CNO decreased the membrane potential of $hM4D_i$ neurons (rest = −67.2 ± 2.8 mV; CNO = −74.0 ± 3.9 mV; paired *t* test, **p* < .05; n.s., nonsignificant; *n* = 7) that recovered following washout (washout = −68.8 ± 2.5 mV; paired *t* test, *p* > .05). mPFC, medial prefrontal cortex.

nonspecific postsynaptic effects on mPFC neurons, we measured action potentials and found that the spiking of both neuronal types was not altered by CNO (both *p*s > .05; Figure 2C, D). In addition, there were no differences in sEPSC frequency in PNs following CNO bath application in slices from control animals (*p* > .05; Figure 2E, G). Hyperpolarization of $hM4D_i$-expressing neurons involves activation of G protein–coupled inwardly rectifying potassium (GIRK) channels at the soma (28,29), but the mechanisms of axonal inhibition remain uncharacterized. To assess the contribution of presynaptic GIRK channels to the CNO's effect on sEPSC frequency, again we used MD-$hM4D_i$ animals. When we included tertiapin-Q (tert-Q, 100 nM), a nonspecific GIRK channel inhibitor, in the bath, we found that the decrease in sEPSC frequency was occluded in PNs. Interestingly, in the presence of tert-Q, CNO increased sEPSC frequency (*p* > .05; Figures 2F, H), suggesting that when GIRK channels are inhibited, activation of $hM4D_i$ receptors may lead to a different downstream signaling cascade. We did not observe any differences in sEPSC amplitude in response to tert-Q, indicating that the increase in sEPSC frequency is likely mediated presynaptically (*p* > .05; Supplemental Figure S1D).

Decreasing MD Activity Disrupts the E/I Ratio in mPFC PNs

To investigate how decreasing MD afferent activity affects intra-mPFC E/I balance, we recorded evoked EPSCs (eEPSCs) and evoked inhibitory postsynaptic currents (eIPSCs) and determined the ratio of the two amplitudes from individual neurons (Figure 3B). Paired-pulse stimuli were delivered in layer II/III, and layer V PNs were clamped at −60 and 0 mV (the reversal potentials for $GABA_A$ and alpha-amino-3-hydroxy-5-methyl-4-isoxazole propionic acid [AMPA]-mediated currents, respectively) to evoke EPSCs and IPSCs. Following inhibition of MD terminals with CNO, there was no difference in the eEPSC amplitude (*p* > .05; Figure 3C); however, the eIPSC amplitude was significantly reduced (*p* = .022), resulting in a shift in the E/I ratio (*p* = .002; Figure 3D). However, there was no difference in the paired-pulse ratio in either eEPSCs or eIPSCs (both *p*s > .05; Figure 3E), suggesting no changes in intra-mPFC presynaptic release probability.

Given the selective reduction in eIPSC amplitude, we hypothesized that MD afferents provide stronger stimulation to GABAergic interneurons, which would be reflected in spontaneous IPSCs (sIPSCs) in mPFC PNs. Following bath application of CNO in mPFC slices, we observed significant reductions in sIPSC frequency (*p* = .034; Figure 3F) but no differences in sIPSC amplitude (Supplemental Figure S1). Next, we measured the average tau in the remaining sIPSCs and observed that the time constant was significantly longer in comparison with control animals (*p* = .001; Figure 3F). The predominant $GABA_A$ receptor ($GABA_AR$) subtype present in the adult rat brain is the α1-$GABA_AR$ (31), which is

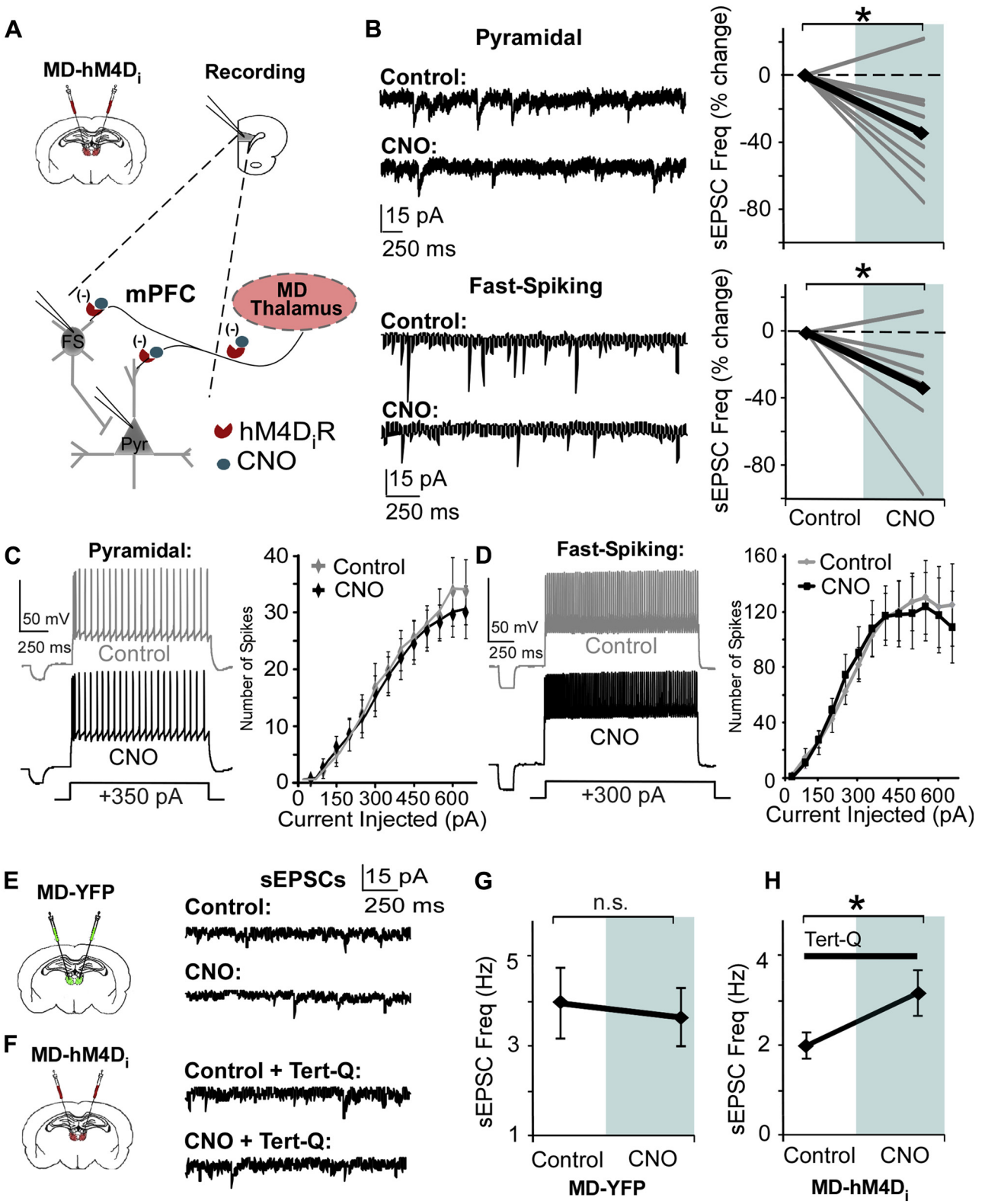


Figure 2. Bath application of clozapine-*N*-oxide (CNO) in the medial prefrontal cortex (mPFC) reduces glutamate release from mediodorsal (MD) presynaptic terminals. **(A)** Strategy for decreasing thalamic activity by inhibiting MD terminals in the mPFC. Graphs show a bilateral injection of the CaMKIIα-hM4D-mCherry or CaMKIIα-eYFP (yellow fluorescent protein) virus and patch-clamp recording in mPFC slices. **(B)** Bath application of 1 μM CNO signficantly

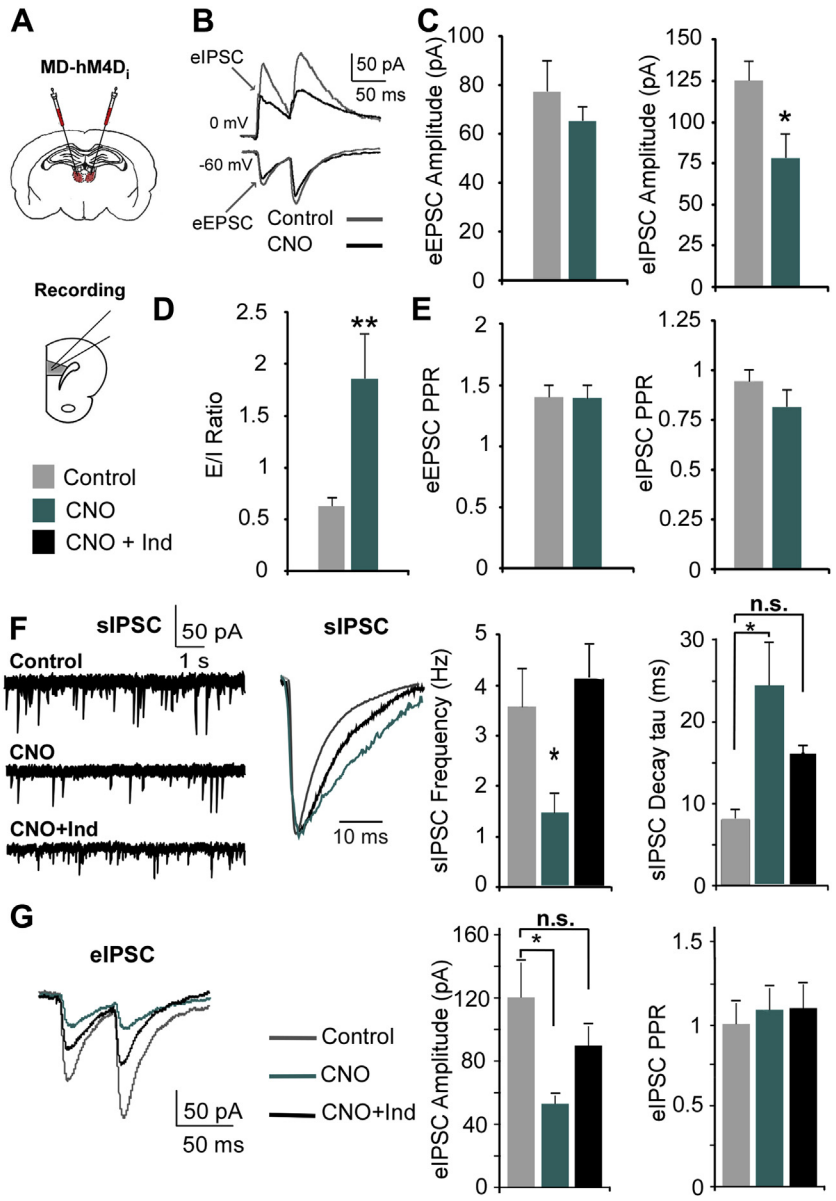


Figure 3. Mediodorsal (MD) inhibition alters medial prefrontal cortex excitation/inhibition (E/I) ratio by decreasing gamma-aminobutyric acidergic signaling, which is rescued by indiplon (Ind). **(A)** The MD was transfected with the inhibitory CaMKIIα-hM4D-mCherry virus, and medial prefrontal cortex slices were collected for recordings 3 weeks post-injection. **(B)** Excitatory postsynaptic currents (EPSCs) and inhibitory postsynaptic currents (IPSCs) were evoked by stimulating layer II/III with paired pulses. **(C)** The evoked IPSC (eIPSC) amplitude, but not the evoked EPSC (eEPSC) amplitude, was significantly decreased by clozapine-*N*-oxide (CNO) (EPSC: control = 77.58 ± 12.82 pA; CNO = 65.18 ± 5.87 pA; Student's *t* test, $^*p < .05$; control $n = 11$, CNO $n = 10$; IPSC: control = 125.3 ± 12.23 pA; CNO = 77.9 ± 15.05 pA; Student's *t* test, $p < .05$). **(D)** Decreasing MD activity increases the E/I ratio (eEPSC/eIPSC amplitude, control = 0.63 ± 0.08; CNO = 1.86 ± 0.43; Mann-Whitney test, $^{**}p < .01$). **(E)** There were no changes in the paired-pulse ratio (PPR; amplitude of the second pulse over the first pulse) in either the eEPSC or eIPSC (Student's *t* test, both *p*s $> .05$). **(F)** The spontaneous IPSC (sIPSC) frequency was decreased by CNO and rescued by coapplication with Ind (1 μM, control = 3.61 ± 0.73 Hz; CNO = 1.49 ± 0.36 Hz; CNO + Ind = 4.13 ± 0.63 Hz; analysis of variance followed by Tukey's post hoc, $F_{2,25} = 6.004$, $^*p < .05$; *n*s = 10 and 8 for control and CNO, respectively). CNO also increased the average decay of the sIPSCs, which was partially rescued by Ind (tau; sIPSCs: control = 7.912 ± 1.26 ms; CNO = 24.50 ± 5.04 ms; CNO + Ind = 15.97 ± 1.90 ms; analysis of variance followed by Tukey's post hoc, $F_{2,24} = 8.91$, $^{**}p < .01$). **(G)** Ind rescued the decreased eIPSC amplitude following CNO administration (control = 120.3 ± 22.0 pA; CNO = 53.0 ± 5.08 pA; CNO + Ind = 89.8 ± 12.1 pA; analysis of variance followed by Tukey's post hoc, $F_{2,27} = 5.18$, group effect $p = .012$, $^*p < .05$; control $n = 10$, CNO $n = 10$, CNO + Ind = 10). n.s., nonsignificant.

characterized by a fast decay. Subunit composition of $GABA_A$Rs confers the decay kinetics of IPSCs (32,33); thus, given the larger tau, we hypothesized that there was reduced activation of α1-$GABA_A$Rs. To examine this, we coapplied CNO and indiplon, an α1-$GABA_A$R positive allosteric modulator, and observed a rescue of sIPSC frequency as well as a partial rescue of the sIPSC decay compared with control animals ($p > .05$ for both). To

decreases spontaneous excitatory postsynaptic current (sEPSC) frequency in pyramidal neurons (PNs) and fast-spiking (FS) interneurons (pyramidal, CNO = −34.8% ± 9.9; FS, CNO = −33.3% ± 12.7; paired *t* test, both $^*p < .05$; pyramidal $n = 9$, FS $n = 7$; data shown as percentage change from baseline). **(C, D)** Spike number in response to depolarizing current injections is not altered by CNO in both PNs and FS interneurons (repeated-measures analysis of variance for final three current injections, pyramidal, control = 8.3 ± 0.76 pA; CNO = 8.3 ± 0.91 pA; paired *t* test, $p > .05$; FS, control = 18.3 ± 1.64 pA; CNO = 16.6 ± 1.64 pA; paired *t* test, $p > .05$; pyramidal cells $n = 9$, FS interneurons $n = 9$). **(E)** Left: Animals received an injection of the control virus in the MD. Right: Representative sEPSCs in mPFC pyramidal cells before and after bath application of CNO. **(F)** Left: Animals received an injection of the hM4D virus in the MD. Right: Representative sEPSCs in mPFC pyramidal cells before and after CNO, with tertiapin-Q (Tert-Q; 100 nM) included in the bath. **(G)** There was no difference in sEPSC frequency before and after CNO in mPFC PNs in animals injected with the control virus in the MD (control = 3.96 ± 0.79 Hz; CNO = 3.64 ± 0.66 Hz; paired *t* test, $p > .05$). **(H)** Including Tert-Q in the bath solution occludes the decrease in sEPSC frequency **(B)**, and sEPSC frequency increases with CNO in mPFC PNs in animals injected with the hM4D virus in the MD (control = 2.00 ± 0.29 Hz; CNO = 3.17 ± 0.51 Hz; paired *t* test, $p > .05$). n.s., nonsignificant.

measure whether indiplon could rescue the eIPSC amplitude, we recorded eIPSCs in PNs (Figure 3G). We found that CNO decreased the eIPSC amplitude, which was rescued by indiplon (p = .012), although there were no differences between groups in paired-pulse ratio ($p > .05$). Similar reductions in GABAergic signaling were observed following systemic CNO administration (Supplemental Figure S2).

Decreasing MD Activity Leads to Deficits in WM That Are Rescued by Indiplon

Given the consistency of WM impairments following MD lesions (34), this provided an ideal paradigm in which to probe the contribution of mPFC disinhibition to WM deficits. We used a delayed nonmatch-to-sample paradigm, where rats were trained to alternate for a food reward in a T maze (Figure 4A). Animals in the control groups (MD-hM4D$_i$ animals treated with saline [MD-hM4D$_i$-SAL] and MD-YFP animals treated with saline or CNO [MD-YFP-SAL and MD-YFP-CNO, respectively]) exhibited no differences in training or testing, so these groups were pooled (see Supplement). These animals were initially compared with MD-hM4D$_i$ animals treated with CNO (MD-hM4D$_i$-CNO; 3 mg/kg). When we measured the learning ability of these groups, there were no differences in task acquisition (p = .352; Figure 4A) prior to any drug treatment. However, when we administered CNO to reduce MD activity and quantified performance, we found a significant group effect at the 60-second delay interval (analysis of variance, p = .033). Post hoc analyses revealed that MD-hM4D$_i$-CNO animals performed worse in comparison with control animals at the longest delay (p = .034; Figure 4B). Given the ability of indiplon to ameliorate GABAergic deficits observed during whole-cell recordings, we treated rats with both CNO and indiplon (3 and 1 mg/kg, respectively [MD-hM4D$_i$-CNO+Ind]), and animals were indistinguishable from control animals at the 60-second delay (p = .883). Together, these data suggest that MD disruption may alter WM through GABAergic hypofunction in the mPFC. In addition, naïve rats treated with indiplon (naïve-Ind) exhibited no differences in performance in comparison with control rats.

Expression of a Novel DREADD Construct

The concurrent findings of decreased GABAergic signaling and WM deficits, along with the ability to rescue these deficits by treatment with a GABAergic positive allosteric modulator, following MD silencing suggest causal links among these phenomena. To explore this with regional and cellular specificity, we designed and used a novel DREADD construct, where an hM3D$_q$ DREADD was inserted into a PV-GFP viral vector (35). Following injection of the PV-hM3D$_q$-GFP into the mPFC, we observed robust GFP staining in the prelimbic mPFC (Figure 5A). To determine whether the construct was expressed in PVIs, we quantified the amount of colocalization with a PV antibody. We found that the hM3D$_q$ DREADD (green) was expressed in approximately 82% of PV-labeled cells (red; colocalization: orange; Figure 5B), while approximately 67% of hM3D$_q$-tagged neurons were PV labeled. Using whole-cell

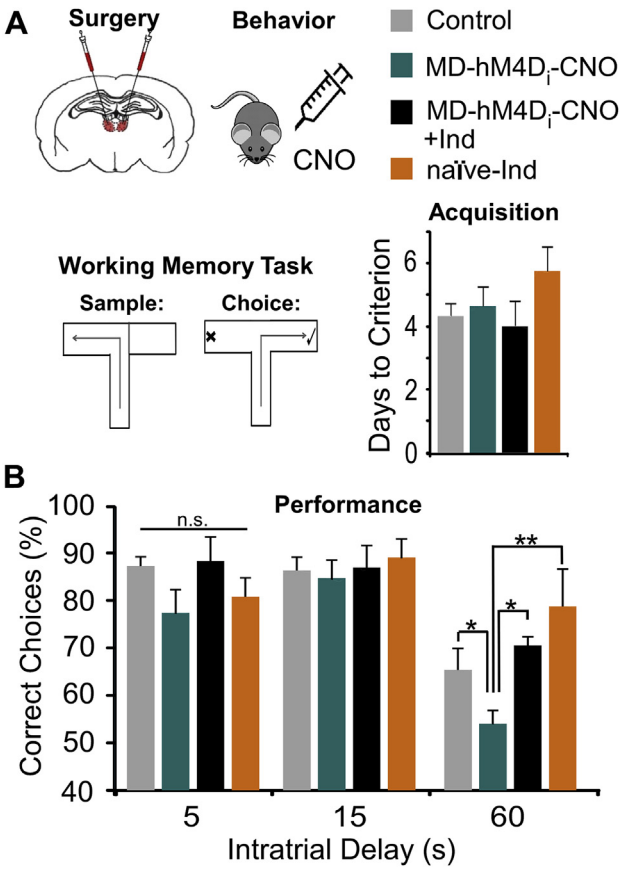


Figure 4. Working memory impairment induced by mediodorsal (MD) inhibition is rescued by the gamma-aminobutyric acidergic positive allosteric modulator, indiplon (Ind). **(A)** Animals received a bilateral transfection of the MD, were treated systemically with saline, clozapine-*N*-oxide (CNO), indiplon, or CNO + indiplon and were tested on a T-maze task. There were no differences in days required to acquire the task (analysis of variance, $F_{3,29}$ = 1.134, $p > .05$; control n = 11, MD-hM4D$_i$-CNO n = 5, MD-hM4D$_i$-CNO+Ind n = 6, naïve-Ind n = 4). **(B)** MD inhibition (MD-hM4D$_i$-CNO) impaired working memory at the 60-second delay interval but not at the 5- and 15-second delay intervals. This deficit was ameliorated by treating rats with Ind (MD-hM4D$_i$-CNO+Ind), whereas Ind alone (naïve-Ind) did not disrupt performance (repeated-measures analysis of variance followed by Tukey's post hoc, $F_{3,20}$ = 3.55, $^*p < .05$, $^{**}p < .01$). n.s., nonsignificant.

recordings, about 70% of hM3D$_q$-labeled neurons exhibited a fast-spiking firing pattern (Supplemental Figure S3). Correspondingly, activating transfected neurons by bath application of CNO caused a significant increase in sIPSC frequency in layer V PNs (p = .041; Figure 5C).

Pharmacogenetic Activation of PVIs Rescues E/I Ratio in mPFC PNs

To explore whether activation of PVIs could restore E/I ratio deficits observed previously, we combined our previous hM4D$_i$ injection into the MD with a bilateral injection of the PV-hM3D$_q$-GFP virus or a control vector into the mPFC (Figure 5D). Identical to previous observations, there were no differences

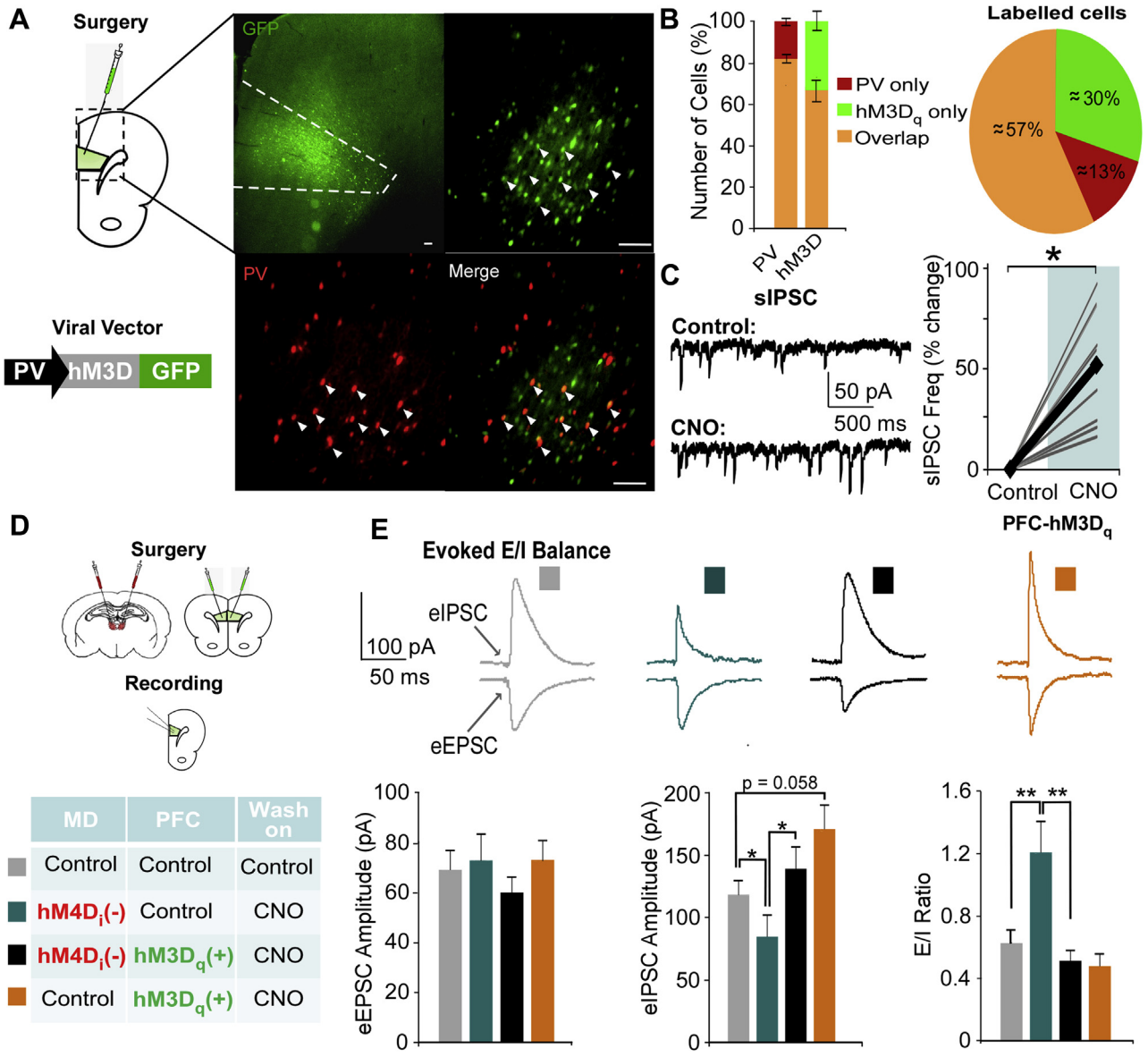


Figure 5. Pharmacogenetic activation of parvalbumin interneurons rescues excitation/inhibition (E/I) ratio. **(A)** Animals received an injection of the excitatory parvalbumin (PV)-hM3D$_q$-GFP (green fluorescent protein) vector in the medial prefrontal cortex (mPFC). Costaining with a PV-antibody (red) revealed colocalization (orange, arrowhead) with the PV-hM3D$_q$-GFP vector (primary: rabbit anti-PV, 1:2,000, Abcam; secondary: DyLight 594–conjugated goat anti-rabbit, 1:500, Jackson ImmunoResearch Laboratories). **(B)** Cells were counted, and the amounts of PV, hM3D$_q$, and overlapping cells were quantified. **(C)** Pyramidal neurons exhibited a signficant increase in spontaneous inhibitory postsynaptic current (sIPSC) frequency following bath application of clozapine-*N*-oxide (CNO) control = 4.99 ± 1.70 Hz, CNO = 6.73 ± 1.99 Hz; an average of > 50% increase, paired *t* test, $^*p < .05$; $n = 10$; data shown as percentage change from baseline. **(D)** Animals received a bilateral transfection of the mediodorsal thalamus (MD) and mPFC with the combinations designated in the table. **(E)** Single pulses were delivered to layer II/III to evoke excitatory postsynaptic currents (EPSCs) and IPSCs in each group. The evoked IPSC (eIPSC) amplitude was significantly decreased by inhibiting MD activity (teal), and this was restored by activating parvalbumin interneurons (black, Kruskal-Wallis test followed by post hoc analyses, $\chi^2_3 = 11.332$, $^*p < .05$, $^{**}p < .01$; MD-Con-PFC-Con $n = 15$, MD-hM4D-PFC-Con $n = 15$, MD-hM4D-PFC-hM3D $n = 19$, MD-Con-PFC-hM3D $n = 13$). MD inhibition alone (orange, MD-Con-PFC-hM3D) also increased the E/I ratio, which was rescued by activating mPFC parvalbumin interneurons (MD-hM4D-PFC-hM3D, Kruskal-Wallis test, $\chi^2_3 = 10.438$, $^*p < .05$, $^{**}p < .01$, $^{***}p < .001$).

across groups in the eEPSC amplitude ($p = .715$; Figure 5E), but there were significant differences in the eIPSC amplitude and E/I ratio (eIPSC, $p = .010$; E/I ratio, $p = .015$). Inhibiting MD activity selectively decreased the eIPSC amplitude (MD-hM4d-PFC-Con, $p = .029$) and increased the E/I ratio ($p = .008$). However, activation of PVIs restored the eIPSC amplitude and normalized the E/I ratio (MD-hM4D-PFC-hM3D, comparison with control animals, $p = .811$ and $p = 1.000$, respectively). In animals where we activated PVIs alone (MD-Con-PFC-hM3D), they exhibited a nonsignificant trend toward an increased

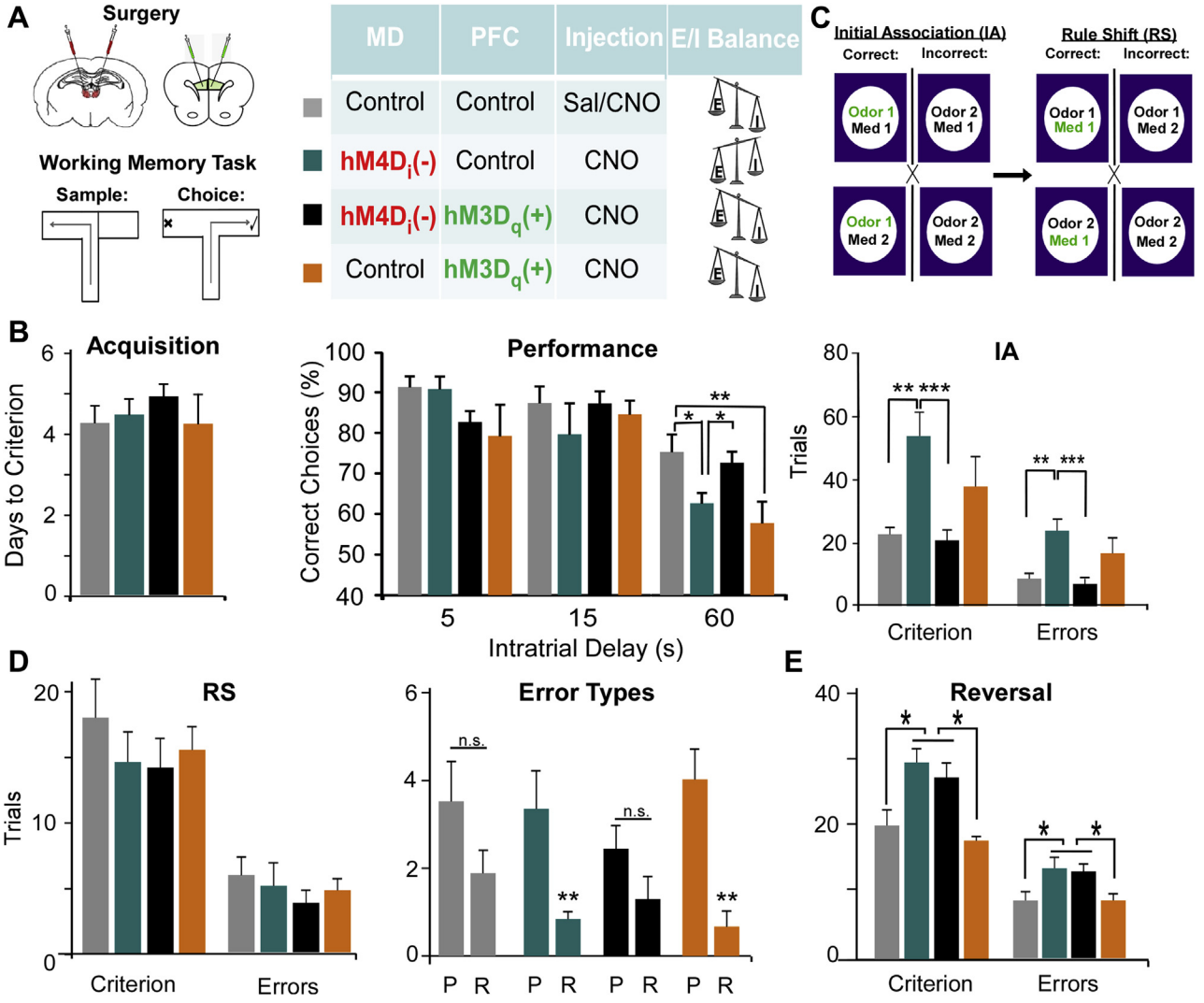


Figure 6. The mediodorsal (MD) regulates working memory and select components of cognitive flexibility through modulation of parvalbumin interneurons (PVIs) in the medial prefrontal cortex (mPFC). **(A)** Rats received a bilateral injection of viruses in the MD and mPFC with the viral combinations designated in the diagram. **(B)** MD inhibition (teal) impaired working memory at the 60-second delay interval, and this was rescued by activation of PVIs (black), while activation of PVIs alone (orange) impaired performance (analysis of variance [ANOVA] followed by Dunnet's post hoc test, $F_{3,24} = 4.493$, $^{*}p < .05$, $^{**}p < .01$, MD-Con-PFC-Con $n = 9$, MD-hM4D-PFC-Con $n = 7$, MD-hM4D-PFC-hM3D $n = 8$, MD-Con-PFC-hM3D $n = 5$). **(C)** Animals were trained to discriminate between scents and digging media to obtain a food reward. MD-hM4D-PFC-Con rats were impaired at learning the initial association (IA) and made more errors, but this was rescued by mPFC PVI activation MD-hM4D-PFC-hM3D. Activating PVIs alone, MD-Con-PFC-hM3D increased trials to criterion and errors (trials to criterion: ANOVA followed by Tukey's post hoc, $F_{3,24} = 6.861$; errors: ANOVA followed by Tukey's post hoc, $F_{3,24} = 6.542$, $^{**}p < .01$, $^{***}p < .001$, MD-Con-PFC-Con $n = 8$, MD-hM4D-PFC-Con $n = 7$, MD-hM4D-PFC-hM3D $n = 7$, MD-Con-PFC-hM3D $n = 6$). **(D)** During the rule shift (RS), there was no difference in trials to criterion when all errors were pooled (ANOVA, criterion $F_{3,24} = 0.632$, errors $F_{3,24} = 0.462$). Only the MD-hM4D-PFC-Con and MD-Con-PFC-hM3D groups exhibited an increase in perseverative (P) errors compared with random (R) errors (Mann-Whitney test, $^{**}p < .01$). **(E)** There was an increase in trials to criterion and errors during the reversal following MD inhibition, which was not rescued by mPFC PVI activation (trials to criterion: ANOVA, $F_{3,17} = 4.720$; errors: ANOVA, $F_{3,17} = 4.947$, $^{*}p < .05$, MD-Con-PFC-Con $n = 4$, MD-hM4D-PFC-Con $n = 7$, MD-hM4D-PFC-hM3D $n = 10$, MD-Con-PFC-hM3D $n = 5$). CNO, clozapine-*N*-oxide; E/I, excitation/inhibition; n.s, nonsignificant.

eIPSC amplitude ($p = .058$) but not an altered E/I ratio ($p = .981$) ex vivo.

Elevating mPFC PVI Activity Restores Certain Behavioral Deficits Induced by MD Inhibition

Rats received the same pattern of injections as described above, and we assessed WM (Figure 6). Similarly, while the shorter delays of 5 and 15 seconds were spared (Figure 6B), differences in performance emerged at the 60-second interval. MD inhibition reduced the percentage of correct trials compared with control animals ($p = .029$); however, activating PVIs was sufficient to fully recover this deficit at 60 seconds (comparison with control animals, $p = .524$). Interestingly, activating PVIs alone suppressed normal WM capacity selectively at 60 seconds ($p = .006$).

We assessed animals on a set-shifting task where animals were trained to dig in bowls that varied in either scent (garlic

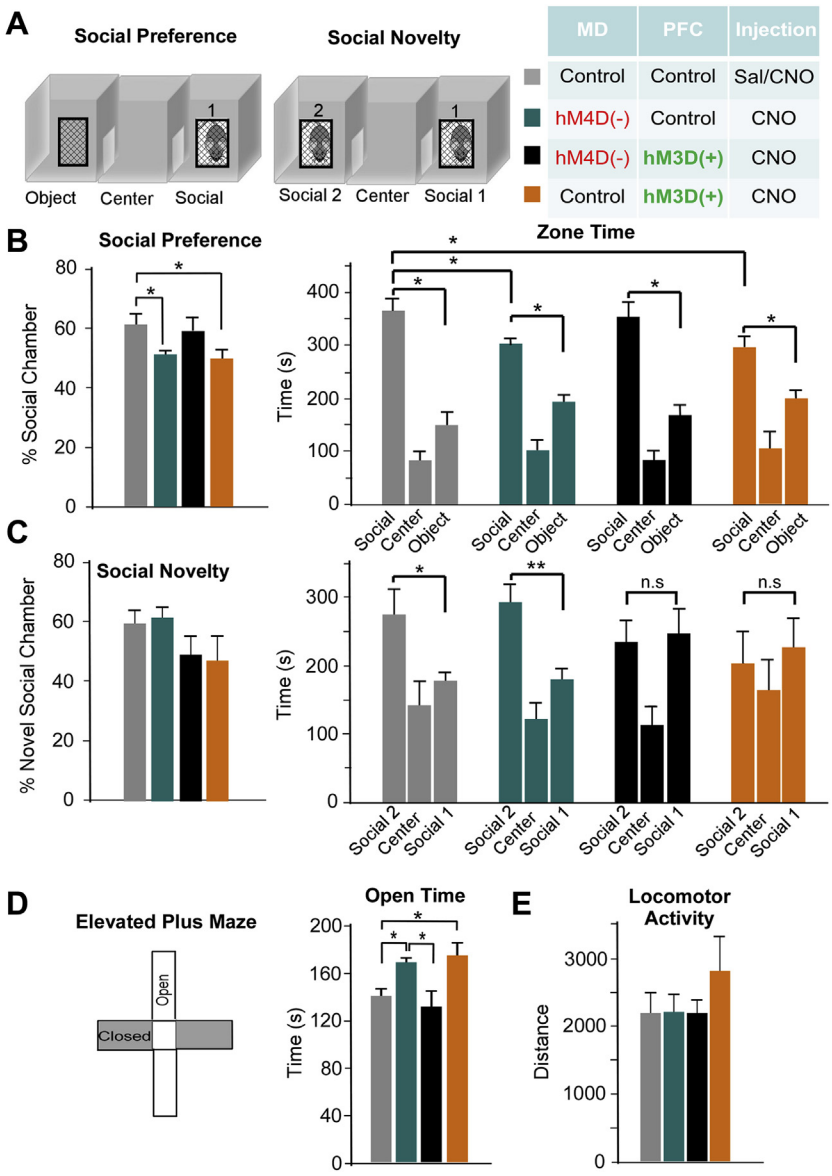
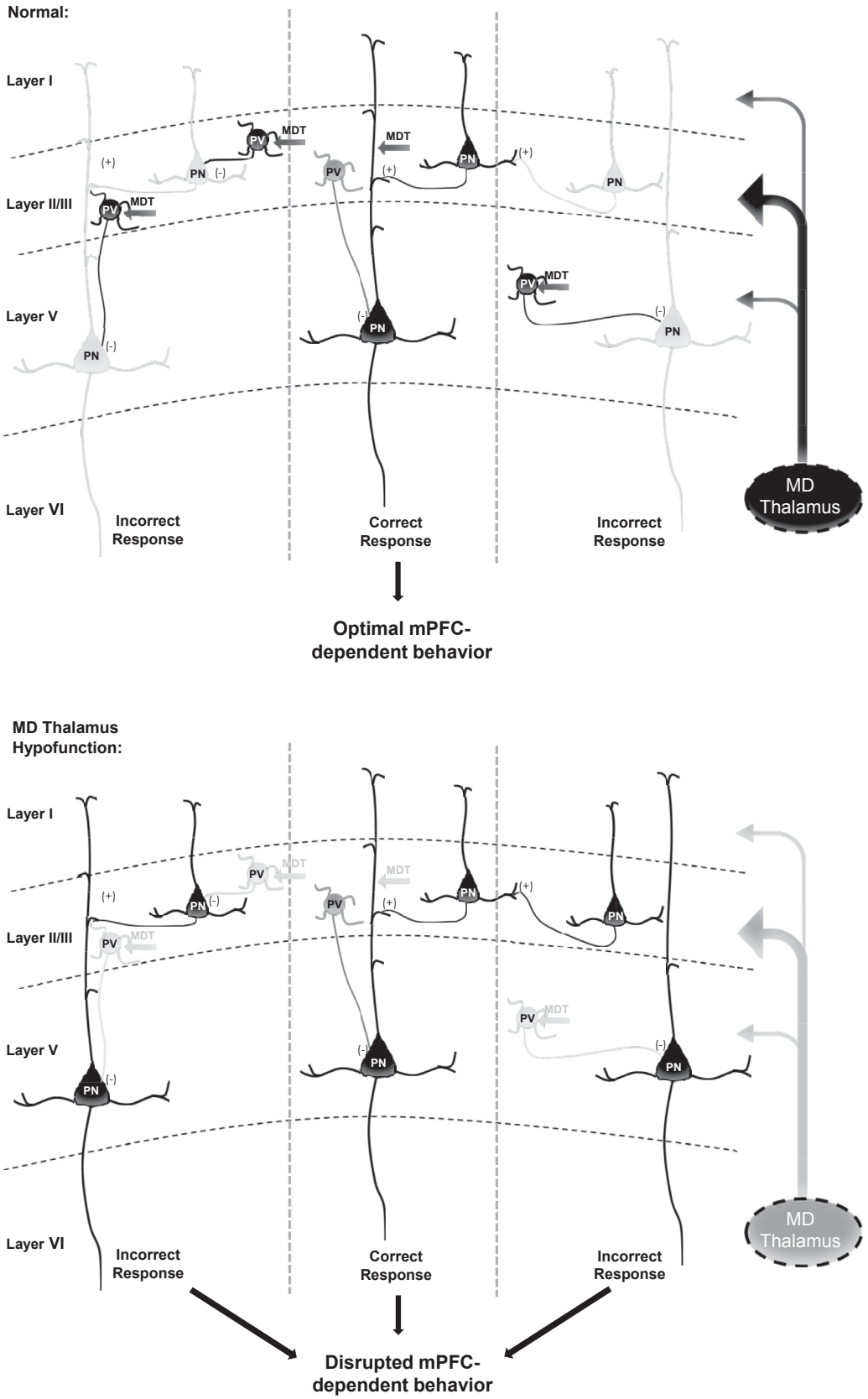


Figure 7. The mediodorsal (MD) thalamus regulates social interaction and anxiety behavior through modulation of parvalbumin interneurons (PVIs) in the medial prefrontal cortex (mPFC). **(A)** Rats were tested on the three-chamber sociability task. During the social preference portion, zone time was measured in the object, center, and social chambers. For social novelty, rats were exposed to a novel rat, and time in each zone was measured. **(B)** MD inhibition (teal) reduced the social preference due to decreased time spent in the social zone. This was rescued by activation of PVIs (black), while activation of PVIs alone (orange) also disrupted social preference (analysis of variance [ANOVA], $F_{3,24} = 2.132$, $^*p < .05$, MD-Con-PFC-Con $n = 6$, MD-hM4D-PFC-Con $n = 7$, MD-hM4D-PFC-hM3D $n = 9$, MD-Con-PFC-hM3D $n = 5$). **(C)** There was no difference in the percentage time spent in the novel social chamber (ANOVA, $F_{3,24} = 1.502$, $p > .05$). In comparison with the control group, MD-Con-PFC-Con, the MD inhibition group, MD-hM4D-PFC-Con, showed a similar preference in zone time for the novel rat chamber ($^*p < .05$). However, this zone time preference was absent in MD-hM4D-PFC-hM3D and MD-Con-PFC-hM3D rats. **(D)** Left: Rats were tested on elevated plus maze, and time spent in open arms was quantified. Right: MD inhibition, MD-hM4D-PFC-Con, and activation of PVIs, MD-Con-PFC-hM3D, showed a similar increase in open time compared with control rats, MD-Con-PFC-Con (ANOVA, $F_{3,25} = 3.079$ $^*p < .05$), while combined MD inhibition and PVI activation, MD-hM4D-PFC-hM3D, normalized this phenotype. **(E)** There were no differences in locomotor activity across all groups (ANOVA, $F_{3,26} = 0.892$ $p > .05$). CNO, clozapine-*N*-oxide; n.s, nonsignificant.

or coriander) or medium (sand or bedding). Animals first learned an initial association (IA) where a certain scent was consistently rewarded (Figure 6C). Interestingly, dampening MD activity (MD-hM4D-PFC-Con) and activating PVIs alone (MD-Con-PFC-hM3D) disrupted learning the IA, increasing the trials to criterion (comparison with control animals, $p = .004$ and $p = .003$, respectively) as well as the total errors (comparison with control animals, $p = .006$ and $p = .003$, respectively). Similar to WM, combined MD silencing and mPFC PVI activation (MD-hM4D-PFC-hM3D) fully recovered learning of the IA (comparison with controls, $p = .974$). Then, animals needed to learn a rule shift where the digging medium now predicted the location of the food reward. Although there were no differences among groups in the trials to criterion or total errors ($p = .602$ and $p = .711$, respectively) (Figure 6D), only silencing of MD activity (MD-hM4D-PFC-Con) and elevating PVI activity (MD-Con-PFC-hM3D) significantly increased perseverative errors compared with random errors ($p = .005$ and $p = .001$, respectively). Following the rule shift, animals underwent a reversal where the previously unrewarded digging medium indicated the rewarded bowl. Unlike the rule shift, reversal learning is underlain by activity in the MD to orbital frontal cortex (OFC) pathway (36–38). There were significant group differences in trials to criterion ($p = .011$; Figure 6E) and in total errors ($p = .009$). We observed an increase in trials to criterion and errors in MD-inhibited animals (MD-hM4D-PFC-Con) compared with control animals (MD-Con-PFC-Con, $p = .030$ and $p = .025$, respectively), while there were no differences between this group and the rescue group (MD-hM4D-PFC-hM3D, $p > .05$). In addition, as predicted, activation of mPFC PVIs alone did not alter reversals ($p > .05$).


Normal:
Layer I
Layer II/III
Layer V
Layer VI
MDT
PV
PN
(+)
(-)
MD Thalamus
Incorrect Response
Correct Response
Incorrect Response
Optimal mPFC-dependent behavior
MD Thalamus Hypofunction:
Disrupted mPFC-dependent behavior

Next, we explored whether our findings from cognition extended to other behaviors sensitive to mPFC disruption. First, we measured social interaction using a three-chamber sociability task (Figure 7A). We observed that MD-inhibited animals (MD-hM4D-PFC-Con) showed a reduction in social preference (p = .040) (Figure 7B) owing to decreased time in the social chamber compared with control animals (MD-Con-PFC-Con; p = .022). Elevating PVI activity (MD-Con-PFC-hM3D) also reduced social preference (p = .034) (Figure 7B). Similar to the normalizing effects of activating PVIs in MD-inhibited animals on cognition, MD-hM4D-PFC-hM3D rats were not significantly different from control rats in social preference or zone time (p = .713 and p = .535, respectively) (Figure 7B). Although there were no differences among groups in percentage of time spent in the novel social chamber (Figure 7C), we found differences in total zone time between the familiar rat and novel rat chambers only in control animals (MD-Con-PFC-Con, p = .031) and the MD-inhibited rats (MD-hM4D-PFC-Con, p = .002), suggesting that MD inhibition does not disrupt social novelty. However, in MD-hM4D-PFC-hM3D animals, this preference was lost, in contrast to the beneficial effects of this manipulation in all other behavioral measures (p = .798), and the social novelty preference was also absent in MD-Con-PFC-hM3D rats (p = .715) (Figure 7C).

To examine the contribution of changes in anxiety levels to social interaction and novelty deficits, we tested animals on the elevated plus maze. MD-hM4D-PFC-Con- and MD-Con-PFC-hM3D-treated rats showed an increase in open-arm time compared with control rats (MD-Con-PFC-Con), suggesting an anxiolytic effect in these two groups (MD-hM4D-PFC-Con, p = .010; MD-Con-PFC-hM3D, p = .025) (Figure 7D). Activating PVIs normalized the anxiolytic effect of MD inhibition (MD-hM4D-PFC-hM3D, p = .652, comparison with control rats). Finally, we found no baseline changes in the ambulatory distance across all groups during open-field testing (p = .458) (Figure 7E).

DISCUSSION

Using pharmacogenetic inhibition of MD afferents, we decreased MD axonal release in the mPFC and observed significant reductions in inhibitory currents, decreased eIPSC amplitude, and an increased E/I ratio. This corresponded with significant behavioral impairments in WM, set shifting, and social interaction. Furthermore, pharmacological and pharmacogenetic approaches selected to increase GABAergic signaling were sufficient to alleviate physiological and behavioral deficits, highlighting a causal link among MD dysfunction, GABAergic signaling in the mPFC, and behavioral alterations.

With CNO bath application, we observed reduced presynaptic glutamate release from MD axon terminals. This was likely facilitated by GIRK channels, as determined by the occlusion of this effect with application of tert-Q prior to CNO. These findings are consistent with data indicating the presence of presynaptic GIRK channels (39), and their efficacy in reducing glutamate release (40). To our knowledge, this is the first demonstration of a mechanism of action for $hM4D_i$ receptors at presynaptic terminals. The reduction in sEPSCs might not represent relative strength of MD inputs in vivo to each neuronal subtype, and rather was used as a model to evaluate how mPFC excitatory and inhibitory neuronal activity may change in response to MD inhibition. However, the magnitude of the reduction does correspond with recent work suggesting that thalamic afferents provides nearly 30% of all total inputs, outnumbering the total intra-mPFC connections (41).

Disentangling primary deficits in inhibition versus excitation due to homeostatic mechanisms that alter both in disease states remains challenging (42,43). However, E/I balance deficits have been proposed as an etiology of cognitive symptoms in psychiatric diseases such as schizophrenia and autism (44,45), both of which harbor prominent GABAergic deficits (46,47). We found that MD inhibition recapitulated certain core phenotypes by reducing inhibition in layer V PNs with associated decreases in α1-$GABA_AR$-mediated sIPSCs. The selective GABAergic hypofunction observed is likely attributable to distinct properties of thalamocortical synapses to PNs versus PVIs such as AMPA receptor composition or density of presynaptic release sites (48,49). If AMPA receptors on PVIs have larger conductances compared with those on PNs, we would expect that decreasing the activity of thalamocortical inputs may have larger consequences for PVI activity.

GABAergic inhibition is proposed to tighten PN spatial selectivity in the PFC (50), and correspondingly mPFC disinhibition is associated with impaired information processing (51), and spatial tuning and WM deficits (20). Selective WM impairments at longer delays have been observed following pharmacogenetic thalamic inhibition in mice (34) as well as with computational modeling of the consequences of mPFC disinhibition on WM maintenance (52), consistent with our results. To assess the contribution of GABAergic hypofunction to the observed deficits, we treated rats with both CNO and indiplon, a potent α1-$GABA_AR$ positive allosteric modulator (53). Similar to the physiological recovery in GABAergic signaling, we observed a full amelioration of WM performance, illustrating the importance of α1-$GABA_ARs$ in mPFC PNs in mnemonic maintenance at longer delays.

We also employed a novel approach for increasing GABAergic signaling using an excitatory DREADD targeted to mPFC PVIs. Combining this with MD inhibition, we were able to selectively increase the eIPSC amplitude and fully restore the normal E/I balance, with corresponding behavioral augmentation. Importantly, elevating PVI activity normalized all

Figure 8. The mediodorsal (MD) thalamus (MDT) regulates medial prefrontal cortex (mPFC) excitation/inhibition balance to affect cognition. Under normal conditions, the MD thalamus provides a stronger drive to layer II/III parvalbumin (PV) interneurons versus pyramidal neurons (PNs) in the medial prefrontal cortex to maintain a high level of inhibition relative to excitation in layer V PNs. Potentially, this allows for lateral inhibition of functional microcolumnar units representing distracting information, such that only relevant information is fed forward to optimize behaviors such as working memory, cognitive flexibility, and social interaction. However, based on our findings, when MD activity is decreased, activation of parvalbumin interneurons by MD afferents is removed, leading to disinhibition of neurons in microcolumns representing distracting or irrelevant information and disrupting behavior. Dark gray and black represent high levels of activity, whereas light gray indicates reduced or low activity. This working model is based on our data and known projections of the MD and connectivity in the medial prefrontal cortex (10,11,21,22).

observed mPFC-dependent WM and cognitive flexibility impairments in MD-inhibited animals. We predict that high levels of inhibition suppress the activity of functional units of neurons or microcolumns representing distracting information. In concert with the appropriate patterns of excitation, dynamic regulation of these two opposing forces likely supports the maintenance of delay-related neuronal activity and sustains rule representations in the mPFC, as was demonstrated recently (2,4). Enabling excitatory reverberation to be preferentially sustained within microcolumns representing the correct information could allow the mPFC to optimally process incoming task-related information that can be fed forward to drive the appropriate behavior (Figure 8).

Previous work has also linked mPFC E/I balance disruption to impairments in sociability (51,54), and consistent with this, we found that social preference, which was disrupted by MD inhibition, was also ameliorated by increasing PVI activity. We determined that these disruptions in sociability were not due to increased anxiety in the affected groups given that both groups with social interaction deficits exhibited an anxiolytic phenotype on the elevated plus maze. This could suggest increases in risk-taking or impulsive behavior in these groups, but this requires further study.

When we silenced the MD or activated mPFC PVIs prior to a digging-based set-shifting task (26), we found a deficit in learning the IA. This contrasts with previous reports demonstrating no differences in learning simple discriminations following MD or PFC lesions (15,55), but it corresponds with primate research demonstrating the involvement of the MD in encoding and acquisition of strategies (56). In agreement with previous studies, these two groups also showed an increase in perseverative errors compared with random errors (15,55). Our findings also confirm a segregation of function between the MD-mPFC and MD-OFC pathways in mediating extradimensional and intradimensional shifts, respectively (36–38). Future studies exploring the reliance of reversal learning on OFC E/I balance are warranted.

Although increasing mPFC PVI activity was not sufficient to alter the E/I ratio in the slice, it was sufficient to disrupt nearly all behaviors examined. We predict that the effects of $hM3D_q$ receptor activation may be more potent in vivo, mimicking behavioral studies using GABA agonists in naïve animals to induce pharmacological mPFC lesions (57). If so, this highlights a cohesive thread among the physiological and behavioral results: that the successful performance in a broad range of mPFC-dependent behaviors depends critically on the maintenance of proper mPFC E/I balance. Furthermore, disturbances to that precise balance in either direction, such as increasing it through inhibiting thalamic activity or reducing it by overactivating mPFC PVIs, will disrupt mPFC circuit function and behavior.

ACKNOWLEDGMENTS AND DISCLOSURES

This work was supported by the Dean's Fellowship for Themed or Collaborative Research of the Graduate School of Biomedical Sciences and Professional Studies of the Drexel University College of Medicine (to BRF), the National Institutes of Health/National Institute of Mental Health (Grant No. F31MH111361 to BRF and Grant Nos. R01MH085666 and R21MH111609 to W-JG), the Helen S. Vernik Schizophrenia Pilot Research Project from the Department of Psychiatry, Drexel University College of Medicine (to W-JG and BRF), and the NARSAD Independent Investigator Award, 2015 (to W-JG).

BRF and W-JG designed the research, BRF performed the research and analyzed the data, and BRF and W-JG wrote the article.

We thank Sarah Monaco and Yelena Gulchina for comments on the manuscript.

The authors report no biomedical financial interests or potential conflicts of interest.

ARTICLE INFORMATION

From the Department of Neurobiology and Anatomy, Drexel University College of Medicine, Philadelphia, Pennsylvania.

Address correspondence to Wen-Jun Gao, Ph.D., Department of Neurobiology and Anatomy, Drexel University College of Medicine, 2900 Queen Lane, Philadelphia, PA 19129; E-mail: wg38@drexel.edu.

Received Jun 21, 2017; revised Nov 25, 2017; accepted Nov 28, 2017.

Supplementary material cited in this article is available online at https://doi.org/10.1016/j.biopsych.2017.11.033.

REFERENCES

1. Guillery RW, Sherman SM (2002): Thalamic relay functions and their role in corticocortical communication: Generalizations from the visual system. Neuron 33:163–175.
2. Bolkan SS, Stujenske JM, Parnaudeau S, Spellman TJ, Rauffenbart C, Abbas AI, *et al.* (2017): Thalamic projections sustain prefrontal activity during working memory maintenance. Nat Neurosci 20:987–996.
3. Wimmer RD, Schmitt LI, Davidson TJ, Nakajima M, Deisseroth K, Halassa MM (2015): Thalamic control of sensory selection in divided attention. Nature 526:705–709.
4. Schmitt LI, Wimmer RD, Nakajima M, Happ M, Mofakham S, Halassa MM (2017): Thalamic amplification of cortical connectivity sustains attentional control. Nature 545:219–223.
5. Opris I, Santos L, Gerhardt GA, Song D, Berger TW, Hampson RE, *et al.* (2013): Prefrontal cortical microcircuits bind perception to executive control. Sci Rep 3:2285.
6. Swadlow HA, Gusev AG, Bezdudnaya T (2002): Activation of a cortical column by a thalamocortical impulse. J Neurosci 22:7766–7773.
7. Hoover WB, Vertes RP (2007): Anatomical analysis of afferent projections to the medial prefrontal cortex in the rat. Brain Struct Funct 212:149–179.
8. Kuroda M, Ojima H, Igarashi H, Murakami K, Okada A, Shinkai M (1996): Synaptic relationships between axon terminals from the mediodorsal thalamic nucleus and layer III pyramidal cells in the prelimbic cortex of the rat. Brain Res 708:185–190.
9. Thomson AM, Bannister AP (2003): Interlaminar connections in the neocortex. Cereb Cortex 13:5–14.
10. Kuroda M, Murakami K, Oda S, Shinkai M, Kishi K (1993): Direct synaptic connections between thalamocortical axon terminals from the mediodorsal thalamic nucleus (MD) and corticothalamic neurons to MD in the prefrontal cortex. Brain Res 612:339–344.
11. Kuroda M, Murakami K, Kishi K, Price JL (1995): Thalamocortical synapses between axons from the mediodorsal thalamic nucleus and pyramidal cells in the prelimbic cortex of the rat. J Comp Neurol 356:143–151.
12. Isaacson JS, Scanziani M (2011): How inhibition shapes cortical activity. Neuron 72:231–243.
13. Kesner RP, Hunt ME, Williams JM, Long JM (1996): Prefrontal cortex and working memory for spatial response, spatial location, and visual object information in the rat. Cereb Cortex 6:311–318.
14. Stokes KA, Best PJ (1990): Mediodorsal thalamic lesions impair "reference" and "working" memory in rats. Physiol Behav 47:471–476.
15. Block AE, Dhanji H, Thompson-Tardif SF, Floresco SB (2007): Thalamic–prefrontal cortical–ventral striatal circuitry mediates dissociable components of strategy set shifting. Cereb Cortex 17:1625–1636.

16. Ragozzino ME, Detrick S, Kesner RP (1999): Involvement of the prelimbic–infralimbic areas of the rodent prefrontal cortex in behavioral flexibility for place and response learning. J Neurosci 19:4585–4594.
17. Sawaguchi T, Matsumura M, Kubota K (1989): Delayed response deficits produced by local injection of bicuculline into the dorsolateral prefrontal cortex in Japanese macaque monkeys. Exp Brain Res 75:457–469.
18. Auger ML, Floresco SB (2015): Prefrontal cortical GABA modulation of spatial reference and working memory. Int J Neuropsychopharmacol 18:pyu013.
19. Paine TA, Slipp LE, Carlezon WA Jr (2011): Schizophrenia-like attentional deficits following blockade of prefrontal cortex $GABA_A$ receptors. Neuropsychopharmacology 36:1703–1713.
20. Rao SG, Williams GV, Goldman-Rakic PS (2000): Destruction and creation of spatial tuning by disinhibition: $GABA_A$ blockade of prefrontal cortical neurons engaged by working memory. J Neurosci 20:485–494.
21. Rotaru DC, Barrionuevo G, Sesack SR (2005): Mediodorsal thalamic afferents to layer III of the rat prefrontal cortex: Synaptic relationships to subclasses of interneurons. J Comp Neurol 490:220–238.
22. Kuroda M, Yokofujita J, Oda S, Price JL (2004): Synaptic relationships between axon terminals from the mediodorsal thalamic nucleus and gamma-aminobutyric acidergic cortical cells in the prelimbic cortex of the rat. J Comp Neurol 477:220–234.
23. Povysheva NV, Gonzalez-Burgos G, Zaitsev AV, Kroner S, Barrionuevo G, Lewis DA, *et al.* (2006): Properties of excitatory synaptic responses in fast-spiking interneurons and pyramidal cells from monkey and rat prefrontal cortex. Cereb Cortex 16:541–552.
24. Floresco SB, Grace AA (2003): Gating of hippocampal-evoked activity in prefrontal cortical neurons by inputs from the mediodorsal thalamus and ventral tegmental area. J Neurosci 23:3930–3943.
25. Clapcote SJ, Lipina TV, Millar JK, Mackie S, Christie S, Ogawa F, *et al.* (2007): Behavioral phenotypes of Disc1 missense mutations in mice. Neuron 54:387–402.
26. Cho KK, Hoch R, Lee AT, Patel T, Rubenstein JL, Sohal VS (2015): Gamma rhythms link prefrontal interneuron dysfunction with cognitive inflexibility in Dlx5/6(+/−) mice. Neuron 85:1332–1343.
27. Moy SS, Nadler JJ, Perez A, Barbaro RP, Johns JM, Magnuson TR, *et al.* (2004): Sociability and preference for social novelty in five inbred strains: An approach to assess autistic-like behavior in mice. Genes Brain Behav 3:287–302.
28. Armbruster BN, Li X, Pausch MH, Herlitze S, Roth BL (2007): Evolving the lock to fit the key to create a family of G protein-coupled receptors potently activated by an inert ligand. Proc Natl Acad Sci U S A 104:5163–5168.
29. Roth BL (2016): DREADDs for neuroscientists. Neuron 89:683–694.
30. Mahler SV, Vazey EM, Beckley JT, Keistler CR, McGlinchey EM, Kaufling J, *et al.* (2014): Designer receptors show role for ventral pallidum input to ventral tegmental area in cocaine seeking. Nat Neurosci 17:577–585.
31. Fritschy JM, Mohler H (1995): $GABA_A$-receptor heterogeneity in the adult rat brain: Differential regional and cellular distribution of seven major subunits. J Comp Neurol 359:154–194.
32. McClellan AM, Twyman RE (1999): Receptor system response kinetics reveal functional subtypes of native murine and recombinant human $GABA_A$ receptors. J Physiol 515(Pt 3):711–727.
33. Lavoie AM, Tingey JJ, Harrison NL, Pritchett DB, Twyman RE (1997): Activation and deactivation rates of recombinant $GABA_A$ receptor channels are dependent on alpha-subunit isoform. Biophys J 73:2518–2526.
34. Parnaudeau S, O'Neill PK, Bolkan SS, Ward RD, Abbas AI, Roth BL, *et al.* (2013): Inhibition of mediodorsal thalamus disrupts thalamofrontal connectivity and cognition. Neuron 77:1151–1162.
35. Nathanson JL, Jappelli R, Scheeff ED, Manning G, Obata K, Brenner S, *et al.* (2009): Short promoters in viral vectors drive selective expression in mammalian inhibitory neurons, but do not restrict activity to specific inhibitory cell-types. Front Neural Circuits 3:19.
36. Chudasama Y, Robbins TW (2003): Dissociable contributions of the orbitofrontal and infralimbic cortex to Pavlovian autoshaping and discrimination reversal learning: Further evidence for the functional heterogeneity of the rodent frontal cortex. J Neurosci 23:8771–8780.
37. Dias R, Robbins TW, Roberts AC (1996): Dissociation in prefrontal cortex of affective and attentional shifts. Nature 380:69–72.
38. Parnaudeau S, Taylor K, Bolkan SS, Ward RD, Balsam PD, Kellendonk C (2015): Mediodorsal thalamus hypofunction impairs flexible goal-directed behavior. Biol Psychiatry 77:445–453.
39. Ponce A, Bueno E, Kentros C, Vega-Saenz de Miera E, Chow A, Hillman D, *et al.* (1996): G-protein-gated inward rectifier K^+ channel proteins (GIRK1) are present in the soma and dendrites as well as in nerve terminals of specific neurons in the brain. J Neurosci 16:1990–2001.
40. Ladera C, del Carmen Godino M, Jose Cabanero M, Torres M, Watanabe M, Lujan R, *et al.* (2008): Pre-synaptic GABA receptors inhibit glutamate release through GIRK channels in rat cerebral cortex. J Neurochem 107:1506–1517.
41. DeNardo LA, Berns DS, DeLoach K, Luo L (2015): Connectivity of mouse somatosensory and prefrontal cortex examined with trans-synaptic tracing. Nat Neurosci 18:1687–1697.
42. Hoftman GD, Datta D, Lewis DA (2017): Layer 3 excitatory and inhibitory circuitry in the prefrontal cortex: Developmental trajectories and alterations in schizophrenia. Biol Psychiatry 81:862–873.
43. Nelson SB, Valakh V (2015): Excitatory/Inhibitory balance and circuit homeostasis in autism spectrum disorders. Neuron 87:684–698.
44. Gao R, Penzes P (2015): Common mechanisms of excitatory and inhibitory imbalance in schizophrenia and autism spectrum disorders. Curr Mol Med 15:146–167.
45. Rubenstein JL, Merzenich MM (2003): Model of autism: Increased ratio of excitation/inhibition in key neural systems. Genes Brain Behav 2:255–267.
46. Coghlan S, Horder J, Inkster B, Mendez MA, Murphy DG, Nutt DJ (2012): GABA system dysfunction in autism and related disorders: From synapse to symptoms. Neurosci Biobehav Rev 36: 2044–2055.
47. Lewis DA, Curley AA, Glausier JR, Volk DW (2012): Cortical parvalbumin interneurons and cognitive dysfunction in schizophrenia. Trends Neurosci 35:57–67.
48. Hestrin S (1993): Different glutamate receptor channels mediate fast excitatory synaptic currents in inhibitory and excitatory cortical neurons. Neuron 11:1083–1091.
49. Kloc M, Maffei A (2014): Target-specific properties of thalamocortical synapses onto layer 4 of mouse primary visual cortex. J Neurosci 34:15455–15465.
50. Wang XJ, Tegner J, Constantinidis C, Goldman-Rakic PS (2004): Division of labor among distinct subtypes of inhibitory neurons in a cortical microcircuit of working memory. Proc Natl Acad Sci U S A 101:1368–1373.
51. Yizhar O, Fenno LE, Prigge M, Schneider F, Davidson TJ, O'Shea DJ, *et al.* (2011): Neocortical excitation/inhibition balance in information processing and social dysfunction. Nature 477:171–178.
52. Murray JD, Anticevic A, Gancsos M, Ichinose M, Corlett PR, Krystal JH, *et al.* (2014): Linking microcircuit dysfunction to cognitive impairment: effects of disinhibition associated with schizophrenia in a cortical working memory model. Cereb Cortex 24:859–872.
53. Petroski RE, Pomeroy JE, Das R, Bowman H, Yang W, Chen AP, *et al.* (2006): Indiplon is a high-affinity positive allosteric modulator with selectivity for alpha1 subunit-containing $GABA_A$ receptors. J Pharmacol Exp Ther 317:369–377.
54. Selimbeyoglu A, Kim CK, Inoue M, Lee SY, Hong ASO, Kauvar I, *et al.* (2017): Modulation of prefrontal cortex excitation/inhibition balance rescues social behavior in CNTNAP2-deficient mice. Sci Transl Med 9:eaah6733.
55. Birrell JM, Brown VJ (2000): Medial frontal cortex mediates perceptual attentional set shifting in the rat. J Neurosci 20:4320–4324.
56. Mitchell AS, Gaffan D (2008): The magnocellular mediodorsal thalamus is necessary for memory acquisition, but not retrieval. J Neurosci 28:258–263.
57. Yoon T, Okada J, Jung MW, Kim JJ (2008): Prefrontal cortex and hippocampus subserve different components of working memory in rats. Learn Mem 15:97–105.